ELSEVIER

Materials Science and Engineering A254 (1998) 282–295

MATERIALS SCIENCE & ENGINEERING A

Effects of alloying elements on microstructure and fracture properties of cast high speed steel rolls Part I: Microstructural analysis

Keun Chul Hwang [a], Sunghak Lee [a], Hui Choon Lee [b,*]

[a] *Center for Advanced Aerospace Materials, Pohang University of Science and Technology, Pohang 790-784, South Korea*
[b] *Roll Technology Department, Kangwon Industries, Pohang 790-370, South Korea*

Received 17 February 1998

Abstract

A study was made of the effects of alloying elements on microstructural factors of six high speed steel (HSS) rolls manufactured by centrifugal casting method. Particular emphasis was placed on the role of hard carbides located along solidification cell boundary and the type of the martensite matrix. Microstructural observation, X-ray diffraction analysis, and hardness measurement were conducted on the rolls to identify carbides. Various types of carbides were formed depending on the contents of strong carbide forming elements. In the rolls containing the high Cr content, MC carbides inside cells and M_7C_3 carbides along cell boundaries were primarily formed, while in the rolls containing the high W and Mo contents, MC carbides inside the cells and fibrous M_2C carbides in the intercellular regions were dominantly formed. The most important microstructural factor affecting overall roll hardness was the intercellular carbides and their distribution. The effects of alloying elements were analyzed on the basis of the liquidus surface diagram, suggesting that the proper contents of carbon, tungsten, molybdenum, chromium, and vanadium were 1.9–2.0, 3–4, 3–4, 5–7, and 5–6%, respectively.

1. Introduction

High speed steel (HSS), widely used for tools, is characterized of excellent hardness, wear resistance, and high-temperature properties. Recently, HSS has been applied to roll materials in order to make rolled plates have homogeneous thickness and uniform surface during hot rolling, thereby leading to enhanced surface quality of rolled plates and extended roll life [1,2]. These HSS rolls have different microstructure and characteristics from high speed tool steels. When manufacturing tool steels, the cast structure is destroyed in the subsequent deformation such as forging, and the final microstructure after heat-treatment consists of tempered martensite containing fine and well-distributed carbides. In the case of the HSS rolls, the cast structure containing coarse carbides is left, and the matrix alone is changed to tempered martensite after heat-treatment.

The carbon content in the HSS rolls is generally 1.5–2.0%, most of which is combined with such strong carbide formers as V, W, and Mo [3–5]. The rest of carbon, 0.3–0.6%, is contained inside the matrix, and forms lath-type martensite when the carbon content is below 0.4%, while plate-type martensite when it is above 0.4% [6]. Coarse carbides are generally segregated along cell boundaries, therefore, overall roll hardness increases, but fracture toughness tends to deteriorate. In addition, the increased rolling force and the temperature rise and drop due to the contact of rolled plates and coolant result in thermal fatigue cracks, roughening the roll surface, or initiating internal cracks which might lead to unexpected fracture [7,8]. Consequently, the microstructural factors such as size, volume fraction, distribution of coarse carbides, and the characteristics of the martensitic matrix play important roles in enhancing the roll properties.

In this study, attempts are made to identify the correlation between microstructure and mechanical properties of cast HSS rolls. It also intends to present essential conditions in alloy designing and manufactur-

* Corresponding author. Tel.: +82 562 2792715; fax: +82 562 2792399.

0921-5093/98/ - see front matter
PII S0921-5093(98)00626-1

Table 1
Chemical compositions of HSS rolls investigated (wt.%)

Roll	C	W	Mo	V	Cr	Si	Mn	P	S	Ni	Al	W^*_{eq}
A	1.95	1.6	1.7	5.1	5.5	1.0	0.9	≤0.05	≤0.05	1.2	0.02	5.0
B1	1.95	2.0	3.0	3.6	9.0	1.0	0.9	≤0.05	≤0.05	1.2	0.02	8.0
B2	1.95	2.0	3.0	5.0	9.0	1.0	0.9	≤0.05	≤0.05	1.2	0.02	8.0
C1	1.90	5.0	2.5	5.0	5.0	1.0	0.9	≤0.05	≤0.05	1.2	0.02	10.0
C2	1.90	5.0	5.0	5.0	5.0	1.0	0.9	≤0.05	≤0.05	1.2	0.02	15.0
D	1.45	5.0	5.0	5.0	5.0	1.0	0.9	≤0.05	≤0.05	1.2	0.02	15.0

* $W_{eq} = W + 2Mo$; Tungsten equivalent.

ing by investigating the effects of alloying elements. Six rolls were fabricated by varying the contents of C, W, Mo, Cr, and V, and their respective effects on microstructure and hardness were investigated. The rolls were designed in such a way that the formation of homogeneously distributed hard carbides was maximized by adjusting the content of carbon and carbide formers to enhance wear resistance, while minimizing the amount of intercellular carbides. Intensive investigation was conducted on various kinds of carbides to analyze the correlation between microstructural factors and mechanical properties.

2. Experimental

Materials used in this study were six HSS rolls manufactured by centrifugal casting method, whose chemical compositions and tungsten equivalents ($W_{eq} = W + 2Mo$) are listed in Table 1. The basic composition of the rolls is 1.9C–5.0V–5.0Cr–1.OSi–0.9Mn–1.2Ni (wt.%), and the rolls are designed to be able to investigate the effect of tungsten equivalent by varying the contents of W and Mo. Roll-A contains the lowest tungsten and molybdenum contents of 1.6–1.7%. The compositions of other rolls are varied to investigate the effects of other elements: i.e., V and Cr variations in Rolls-B1 and -B2, increased tungsten equivalent in Rolls-C1 and -C2, and reduced carbon in Roll-D. The rolls were manufactured by a laboratory-scale horizontal centrifugal casting apparatus. The melt was charged into the high-speed revolving mold to form a shell part. Prior to solidification, a core part of nodular graphite cast iron was introduced to produce the rolls with 400 mm in diameter (shell thickness of 65 mm) and 600 mm in length. The roll samples were obtained from the shell part, and were austenitized at 980–1100°C, water quenched, and double-tempered at 495–635°C.

The samples were polished and etched in 3% nital, and were observed by an optical microscope and a scanning electron microscope (SEM). Compositions of carbides and the matrix were quantitatively analyzed by energy dispersive spectroscopy (EDS) and wave-length dispersive spectroscopy (WDS). Carbides were examined using Murakami etchant [9] (3 g $K_3Fe(CN)_6$ + 10g NaOH + 100 ml Hz_2O), in which M_2C (black), M_7C_3 (light pink), and M_6C (pink) carbides are selectively etched but not the matrix and MC carbides. The cell size and the volume fraction of respective carbides were quantitatively analyzed using an image analyzer. Additionally, the matrix was deeply etched in an etchant of 5g $FeCl_3$ + 10 ml HNO_3 + 3 ml HCl + 87 ml ethyl alcohol [10] to observe the three-dimensional shape of carbides by an SEM. An X-ray diffractometer was used to confirm the kind of carbides and to measure the amount of retained austenite (γ). Overall bulk hardness of the rolls, microhardness of the matrix, and microhardness of carbides were also measured by a vickers hardness tester under 30 kg, 1 kg, and 10 g loads, respectively.

3. Results

3.1. As-cast microstructure and hardness

Fig. 1(a) through (f) are optical micrographs of the six as-cast HSS rolls. M_7C_3 type or M_2C type carbides are located along solidification cell boundaries, and most of MC type carbides are formed inside cells. In Rolls-B1 and -B2 with the high content of chromium, a large amount of mixture of M_7C_3 and M_2C carbides is found in a network form in the intercellular region (Fig. 1(b) and (c)). In Rolls-C1, -C2, and -D with the high tungsten and molybdenum contents, a number of fibrous (needle-like) M_2C carbides are observed in the intercellular region. In Roll-D, fishbone-like M_6C carbides are also distributed besides M_2C carbides (Fig. 1(f)). MC carbides are relatively uniformly distributed inside the cells in a spherical or a rod-like shape in most of the rolls. In Roll-B1, however, they are concentrated on cell boundaries rather than inside cells because of the low vanadium content (3.6%) (Fig. 1(b)). In the matrices of all the rolls, a mixture of lath-type and plate-type martensites exists. The formation ratio of these two martensites is different depending on the rolls, with more plate-type martensite observed in Rolls-A, -C1, and -C2.

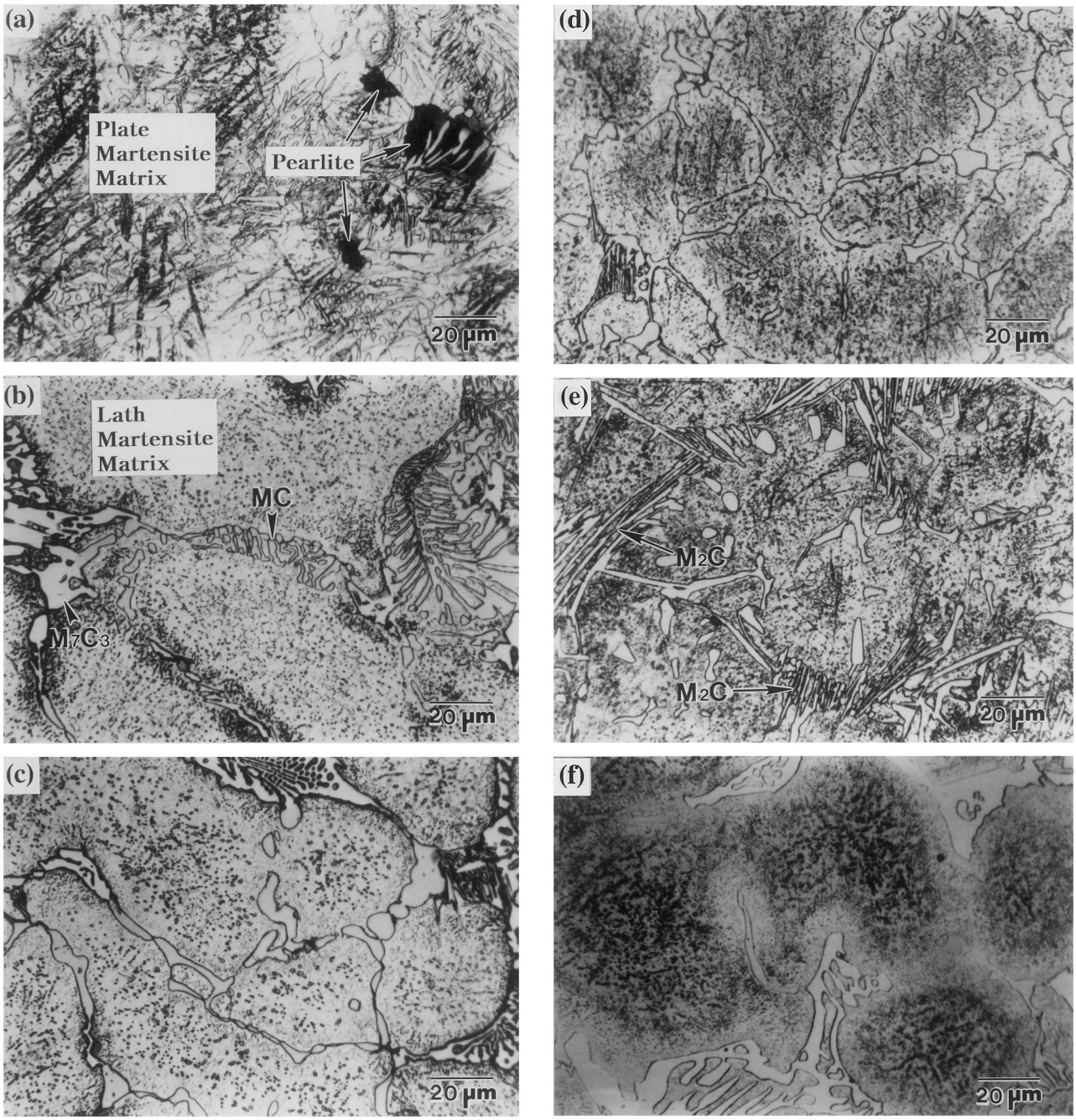

Fig. 1. (a) through (f) Optical micrographs of the shell region of six as-cast HSS rolls. Nital etched.

Fig. 2(a) and (b) are SEM micrographs of the matrices of Rolls-C2 and -D. It can be confirmed that the as-cast matrix is of plate martensite in Roll-C2, whereas lath martensite in Roll-D. Evenly distributed inside the matrix are quite fine spherical carbides. These fine carbides are known as $M_{23}C_6$ precipitated when the rolls are cooled slowly during casting [11]. In the matrix of Roll-A, dark areas can be observed as marked by arrows in Fig. 1(a), and are found to be pearlite by SEM observation (Fig. 2(c)).

Optical micrographs of the rolls etched by Murakami etchant are shown in Fig. 3(a) through (f). A mixture of M_7C_3 (light grey) and M_2C (black) carbides resides in Rolls-B1 and -B2 (Fig. 3(b) and (c)). Due to the higher content of Cr than W and Mo, more M_7C_3 carbides are formed than M_2C carbides. Carbides in Rolls-C1, -C2, and -D are mostly fibrous M_2C carbides (Fig. 3(d) through (f)), with occasional observation of M_6C carbides in Roll-D.

The results of quantitative EDS analyses of MC, M_2C, M_6C, and M_7C_3 carbides formed in Rolls-B2 and -D are shown in Table 2. MC carbides are V-rich

carbides (V_4C_3 in chemical stoichiometry) containing mostly V with small amounts of W, Mo, Cr, and Fe. M_2C and M_6C carbides are carbides containing Mo and W, and M_7C_3 carbides are Cr-containing ones.

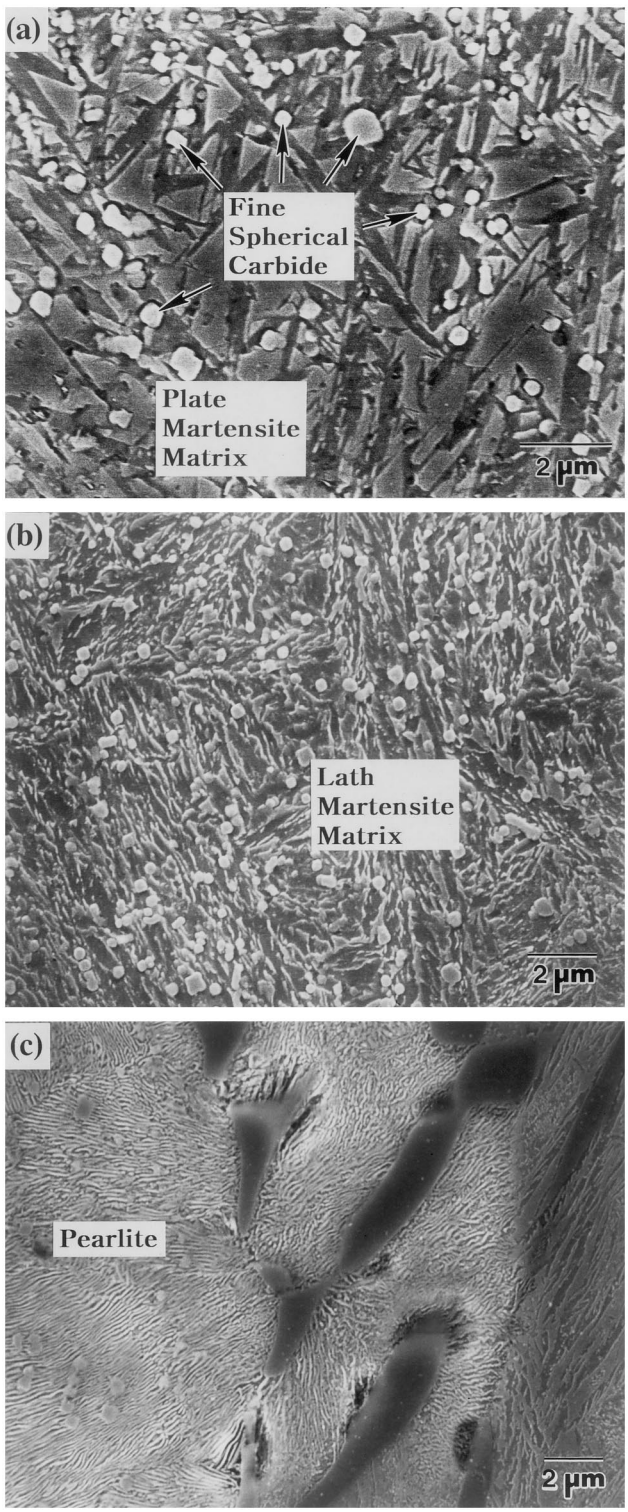

Fig. 2. SEM micrographs of: (a) Roll-C2; (b) Roll-D; and (c) Roll-A; showing the martensitic matrix in the as-cast condition. Note the pearlite structure in (c). Nital etched.

Table 3 shows the microhardness data of these carbides. The hardness of MC carbides formed inside cells is considerably high at 2740 VHN, while those of M_2C, M_6C, and M_7C_3 carbides in the intercellular region are 2230, 1890, and 2380 VHN, respectively, showing much higher hardness than the martensitic matrix (650 VHN). These microhardness values are close to those reported in previous literatures [12–14].

After the matrix and fine carbides were removed by deep-etching method, an X-ray diffraction analysis was conducted on the carbides protruded on the surface, the results of which are shown in Fig. 4(a) through (c). Rolls-A, -B1, and -B2 consist of MC, M_2C, and M_7C_3 carbides (Fig. 4(a)), Rolls-C1 and -C2 of MC and M_2C carbides (Fig. 4(b)), and Roll-D of MC, M_2C, and M_6C carbides (Fig. 4(c)). Fig. 5(a) through (c) show three-dimensional SEM observations of the protruded carbides. The typical shape of M_7C_3 carbides is of brain structure (Fig. 5(a)), while MC carbides of either rod-like (Fig. 5(a)) or coral-like (Fig. 5(b)) shapes grown into cell boundaries from inside cells. M_2C carbides shaped fibrous in Fig. 3(e) are observed in lamellar plates in three-dimension (Fig. 5(b)), and M_6C carbides are typically shaped in fishbone-type with midplanes (Fig. 5(c)).

Table 4 lists the results of quantitative analyses by image analyzer, WDS, and X-ray diffraction methods, respectively, on cell size, volume fraction of carbides, carbon content in the matrix, and volume fraction of retained austenite. Cells in Rolls-A, -B1, and -B2 are sized by 95, 84, and 76 μm, respectively, showing a decrease as tungsten equivalent increases, and the fraction of MC carbides is considerably low at 5%. Although a small amount of M_2C carbides is found in these rolls, they are counted as M_7C_3 in the quantitative analyses of Table 4 because they are usually mixed with M_7C_3. The fraction of M_7C_3 carbides in Rolls-B1 and -B2 containing a large amount of Cr (9%) is high at about 15%, resulting in a considerably higher fraction of overall carbides at around 17–19% than Roll-A's (9.1%). The cell sizes of Rolls-C1 and -C2 containing the increased contents of W and Mo are about 90 μm, and their fraction of MC carbides is 10–12%, larger than Rolls-B1 and -B2's. Due to the large amount of M_2C carbides in Rolls-C1 and -C2, the overall fraction of carbides ranges around 18–24%. The cell sizes of Roll-D, containing the high contents of W and Mo but with the reduced carbon content (1.45%), are the largest at around 110 μm. The fraction of MC carbides is measured to be about 8%, higher than in Rolls-A, -B1, and -B2 but lower than in Rolls-C1 and -C2. In terms of the total carbide fraction, only Roll-A is low at about 9%, while the rest ranges at 18–24%. The carbon content in the matrix of Rolls-A, -C1, and -C2 is high at above 0.6%, but low at below 0.4% in other rolls. These carbon content data are congruent with the morphology of the martensitic matrix as shown in Fig.

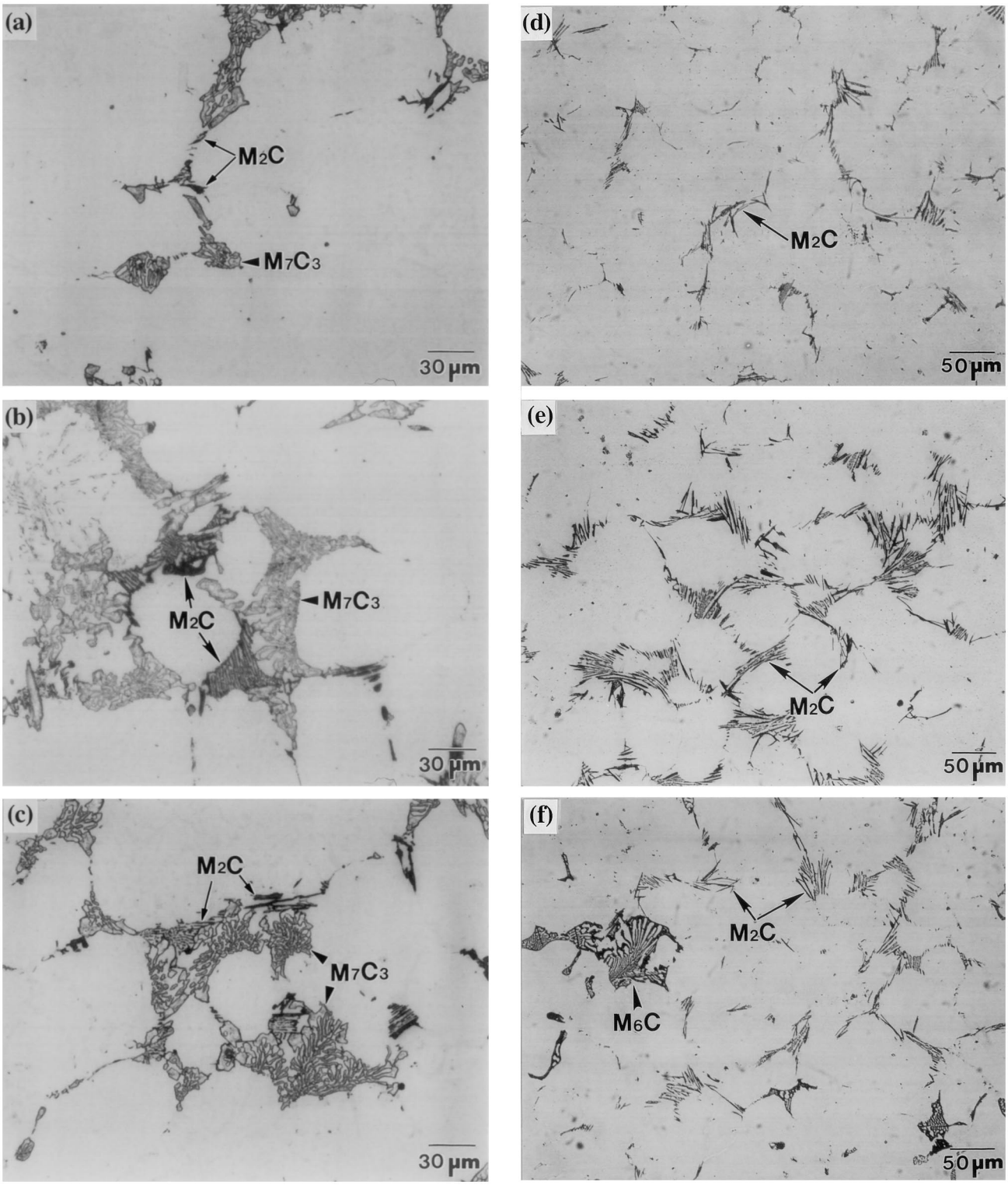

Fig. 3. (a) through (f) Optical micrographs of the shell region of six as-cast HSS rolls. Etched by Murakami etchant.

1(a) through (f). In Rolls-A, -C1, and -C2, plate martensite are mainly observed, whereas mostly lath martensite in the other rolls. The fraction of retained austenite is high at 15–20% in Rolls-A, -C1, and -C2, and low at below 6% in the other rolls, showing a similar tendency to the matrix carbon content.

Table 5 shows the vickers hardness data of the matrix and the overall bulk of the rolls. The matrix hardness is the highest in Rolls-C1 and -C2, followed by Rolls-B1 and -B2. These results are generally similar to those of the matrix carbon content of Table 4. Rolls-C1 and -C2 composed of the plate martensitic matrix have the

Table 2
EDS analysis data of MC, M_2C, M_6C, and M_7C_3 eutectic carbides of as-cast B2- and D-Rolls (wt.%)

Eutectic Carbide	W	Mo	V	Cr	Fe
MC	9.3	4.8	73.5	8.2	4.3
M_2C	36.6	37.1	8.6	11.1	6.5
M_6C	38.7	26.3	5.0	4.4	25.7
M_7C_3	4.4	7.7	11.1	36.9	39.8

highest hardness, and the matrix hardness decreases in the rolls composed of the lath martensitic matrix. Despite the high matrix carbon content and the plate martensitic matrix, Roll-A shows low matrix hardness because of the considerable amount of pearlite in the matrix. The general tendency of overall bulk hardness is almost the same as matrix hardness.

3.2. Post-heat-treatment microstructure and hardness

Fig. 6(a) through (d) are X-ray diffraction results of Roll-C2, showing the process of phase change as it goes through quenching and double-tempering after casting. At the as-cast state, peaks of martensite, MC, and M_2C carbides are dominant, together with a small amount of austenite (Fig. 6(a)). Upon austenitization at 1100°C for 1 h and quenching, peaks of martensite, MC, and M_2C carbides remain, and new peaks of M_6C carbides appear (Fig. 6(b)). Upon quenching, the amount of retained austenite considerably increases. At the tempering temperature of 560°C showing the highest hardness in this roll and at higher (635°C), the peak intensity of retained austenite decreases as the tempering temperature rises, although the peak intensities of other phases do not vary much (Fig. 6(c) and (d)). In addition, the Bragg angle (2θ) of $(110)_\alpha$, the highest peak of martensite, is 43.914° at both as-cast and quenched states, but it increases to 44.202 and 44.376°, respectively, as it goes through double-tempering at 560 and 635°C. This is associated with the phase transformation of martensite into tempered martensite.

Fig. 7(a) and (b) are SEM micrographs showing the decomposition process of M_2C carbides in Roll-C2. Fibrous M_2C carbides at the as-cast state (Fig. 7(a)) are decomposed into MC carbides (black) and M_6C carbides (light grey) after austenitization (Fig. 7(b)). This arises from the peritectoid and eutectoid reaction of $\gamma + M_2C \rightarrow MC + M_6C$; from which the formation of M_6C carbides, as was observed in Fig. 6(b), can be confirmed. The decomposition rate tends to rise with increasing the austenitization temperature. M_2C carbides stay the same in their form even after they are completely transformed into MC and M_6C carbides, therefore, it can be inferred that such properties as resistance to thermal fatigue and fracture toughness are not affected much.

The vickers hardness data of the rolls austenitized at 980–1100°C and double-tempered at 495–635°C are shown in Fig. 8. In all the rolls, the higher the austenitization temperature is, the higher the hardness is. This is because fine $M_{23}C_6$ carbides are dissolved into austenite at higher austenitization temperature, and then austenite is quenched to transform to martensite with the higher hardness. Rolls-A, -B1, and -B2 show the maximum hardness at the tempering temperature of 525°C, and Rolls-C1, -C2, and -D at 550°C. After reaching the maximum hardness, the hardness decreases with increasing the tempering temperature. Also, the maximum hardness tends to show a similar trend to that in the as-cast state shown in Table 5. Unlike in typical high speed tool steels, there is no obvious secondary hardening during tempering. The matrix hardnesses are graphed in Fig. 9(a) and (b) in comparison with the overall hardness of Rolls-C1, and -C2. The matrix hardness is lower than the overall roll hardness, but both show a similar tendency. Thus, it can be found that if the total carbide fraction stays nearly constant, the matrix hardness affects the overall roll hardness to a great extent.

4. Discussion

HSS rolls are generally characterized of much higher hardness and more excellent resistance to wear, oxidization, and roughness by adding strong carbide formers like V, W, Mo, and Cr to form very hard carbides of MC, M_2C, M_6C, and M_7C_3 [4–6,15] than conventional work rolls such as Adamite roll, Ni-grain cast iron roll, and high chromium cast iron roll. However, the large-scale HSS rolls currently manufactured by centrifugal

Table 3
Microvickers hardness data of eutectic carbides and the matrix of as-cast B2- and D-Rolls (load; 10 g)

Location of Indentation	Matrix	MC	M_2C	M_6C	M_7C_3
Microvickers Hardness (VHN)	650	2740	2230*	1890*	2380**

* Vickers hardness measured in D-Roll.
** Vickers hardness measured in B2-Roll.

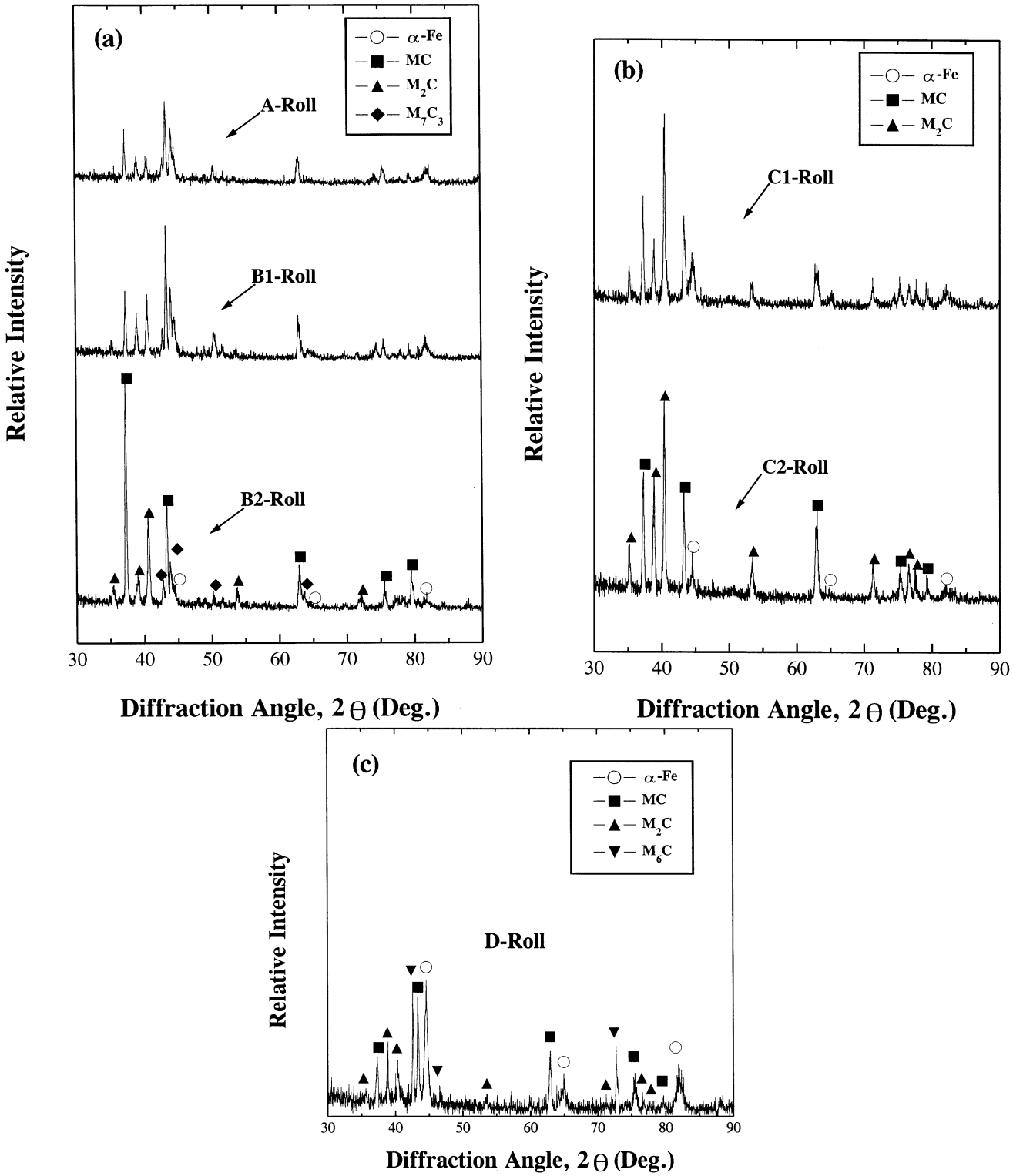

Fig. 4. X-ray diffraction patterns of: (a) Roll-A, -B1, and -B2; (b) Roll-C1 and -C2; and (c) Roll-D, showing peaks of MC, M_7C_3, M_2C, and M_6C eutectic carbides. All the patterns are obtained from the deeply etched specimens, and include α-Fe matrix peaks.

casting retain coarse cell structures and carbides formed during casting because they can not subjected to subsequent forging process [7,8]. Furthermore, the microsegregation developed during solidification is hard to be removed because austenitization can not be performed at very high temperatures.

The properties of HSS rolls are determined by various microstructural factors such as: (1) kind, shape,

volume fraction, and distribution of carbides; (2) characteristics of the martensitic matrix; and (3) solidification cell structure made up of carbides. Carbides directly influence on wear resistance of rolls and surface quality of rolled plates since carbides are very hard. The matrix is related with overall hardness, strength, and fracture toughness of rolls, and plays a sustaining role for hard carbides. The cell size also plays a critical role in determining the overall carbide distribution, directly affecting mechanical properties. Thus, these microstructural factors should be controlled in optimal combinations to manufacture the HSS rolls with excellent properties.

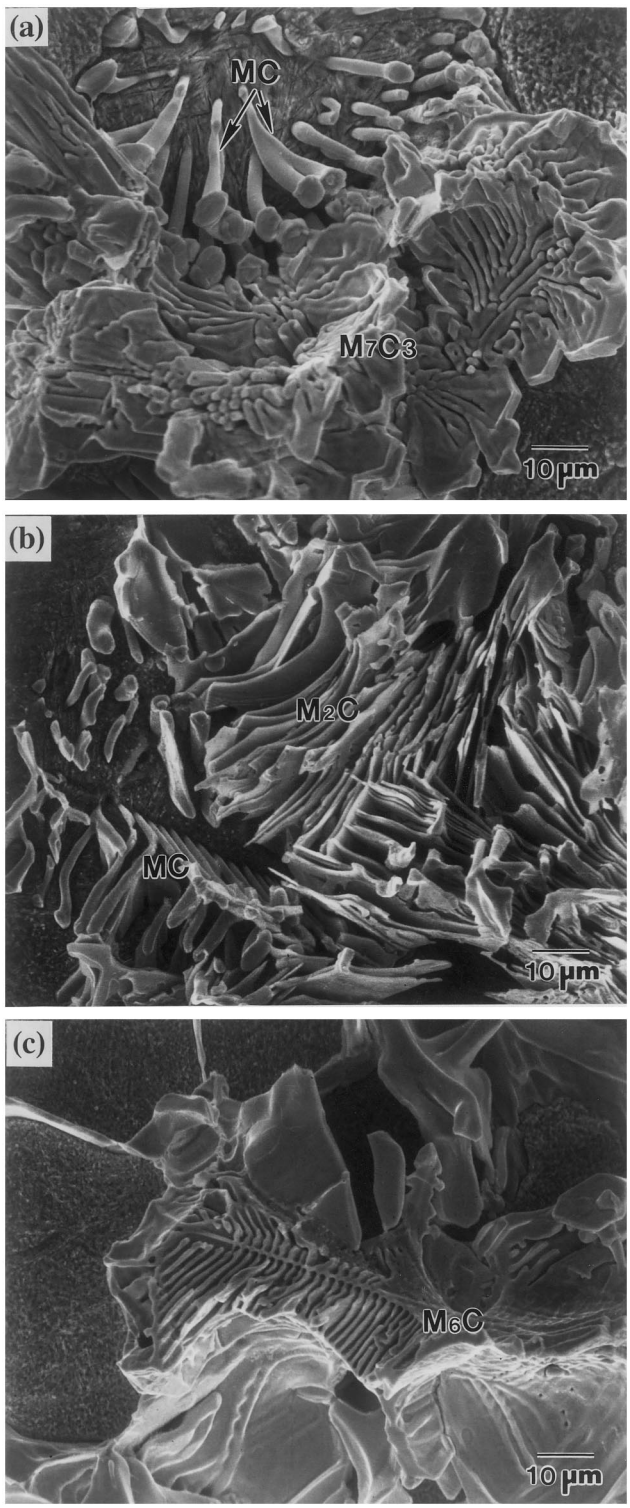

Fig. 5. SEM micrographs of three dimensional morphology of eutectic carbides, showing: (a) a brain structure of M_7C_3 and rod- or coral-like MC carbides in A-Roll; (b) lamellar-type M_2C carbides in Roll-C2; and (c) fishbone-type M_6C carbides in Roll-D.

It is impossible to satisfy all the roll properties at the same time, therefore, considerations should be made of prior properties that have to be satisfied, based on the roll characteristics and the rolling environments. For example, in the roughening stand rolls, resistance to thermal fatigue and oxidization, and high fracture toughness should be prioritized rather than resistance to wear and roughness. On the other hand, the finishing stand rolls require wear resistance and high impact toughness, therefore, rolls should be appropriately designed depending on the rolling conditions. To improve wear resistance, it is recommended to enhance the hardness of the tempered martensitic matrix and to form many hard carbides. When resistance to roughness is to be prioritized, the increase of the contents of W, Mo, and Cr or the addition of Co would be necessary to sufficiently strengthen the matrix. It is also required to add a sufficient amount of Cr to improve resistance to oxidization. For fracture toughness and thermal fatigue properties, rolls should be designed to enhance the carbide distribution and to soften the matrix, often at the expense of deteriorating other properties.

4.1. Formation behavior of carbides as to liquidus surface diagram

In order to analyze the effects of alloying elements added to the HSS rolls, the liquidus surface diagram showing the solidification process, as in Fig. 10, is useful [16]. Although this diagram is concerned with three HSS systems of Fe–5Cr–V–C, Fe–15Cr–V–C, and Fe–5Cr–5W–5Mo–V–C, it can be applied roughly to the alloy compositions of the rolls used in the present study. Fe–5Cr–V–C system corresponds to Roll-A (5.5%Cr), Fe–15Cr–V–C to Rolls-B1 and -B2 (9%Cr), and Fe–5Cr–5W–5Mo–V–C to Rolls-C1, -C2, and -D ($W_{eq} = 10–15$).

According to the solidification theory, the liquidus lines are supposed to always move in the direction of temperature drop. In the case of Roll-A, the liquid phase composition starts from the composition point 'A' of 2%C–5%V, moves to B_1 direction, and forms primary austenite (γ). Upon arriving at B_1, the liquidus line moves along $B_1P'_1$ line, and forms MC carbides by the eutectic reaction of $L \rightarrow \gamma + MC$. In general, the ($\gamma + MC$) eutectic structure independently-nucleates

Table 4
Results of quantitative analysis of as-cast HSS rolls

Roll	Cell size (μm)	Volume fraction of Eutectic carbides (%)					Carbon content in matrix (wt.%)	Volume fractione of retained austenite (%)
		MC	M_2C	M_6C	M_7C_3	Total		
A	95	4.4	—	—	4.7*	9.1	0.73	15.8
B1	84	2.2	—	—	15.4	17.6	0.48	6.3
B2	76	5.0	—	—	14.0*	19.0	0.42	3.5
C1	89	12.3	5.6	—	—	17.9	0.63	19.5
C2	91	10.0	14.0	—	—	24.0	0.62	16.6
D	110	7.7	4.5	5.6	—	17.8	0.35	4.8

* Small amount of M_2C carbides are included in this value.

and grows to form one cell, or grows at the periphery of primary γ. Given that nucleation sites are same, the longer AB_1 and $B_1P'_1$ lines are, the longer it takes for primary γ and (γ + MC) eutectic structure to grow, and the larger the cells get. The cell sizes of Rolls-B1 and -B2 are smaller than that of Roll-A (Table 4) because AB_2 and $B_2P'_2$ lines are short. Especially, the cell size of Roll-B2 is very small at 76 μm because it contains the largest tungsten equivalent among the four rolls, affecting $P_2P'_2$ line to drop a little further down and AB_2 line to get further shortened. Rolls-A, and -B2 containing 5% V have a relatively small amount of MC carbides (4.4–5.0%) because the interval of MC carbide formation is short, whereas the interval of primary γ formation is long. In Roll-B1 containing 3.6% V, the starting solidification point is located below Point A, and causes the interval of primary γ formation to be longer, while that of MC carbides to be shorter. As a result, the amount of MC carbides is reduced (2.2%), and they are distributed mainly in the intercellular region.

The formation of M_7C_3 carbides can also be explained by the liquidus surface diagram. In Roll-A, a large amount of primary γ and (γ + MC) eutectic structure are formed because AB_1 and $B_1P'_1$ lines are long. When the liquidus line reaches at Point P'_1, a small amount of M_7C_3 carbides (about 4.7%) is formed because only a small amount of liquid phase participates in the peritectic and eutectic reaction of L + MC → γ + M_7C_3. However, in Rolls-B1 and -B2, primary γ and (γ + MC) eutectic structure are formed in a small amount because both AB_2 and $B_2P'_2$ lines are short, and many M_7C_3 carbides (about 14.0–15.4%) are formed due to a large amount of remaining liquid phase when the line reaches at Point P'_2. The fraction of total carbides reaches up to about 18–19% in Rolls-B1 and -B2, although it does not exceed over 9% in Roll-A.

Table 5
Vickers hardness of the matrix and the overall bulk of as-cast HSS rolls

Roll	Matrix hardness* (VHN)	Overall bulk hardness** (VHN)
A	569	588
B1	675	667
B2	665	673
C1	691	677
C2	729	722
D	567	627

* Hardness value measured under the load of 1 kg.
** Hardness value measured under the load of 30 kg.

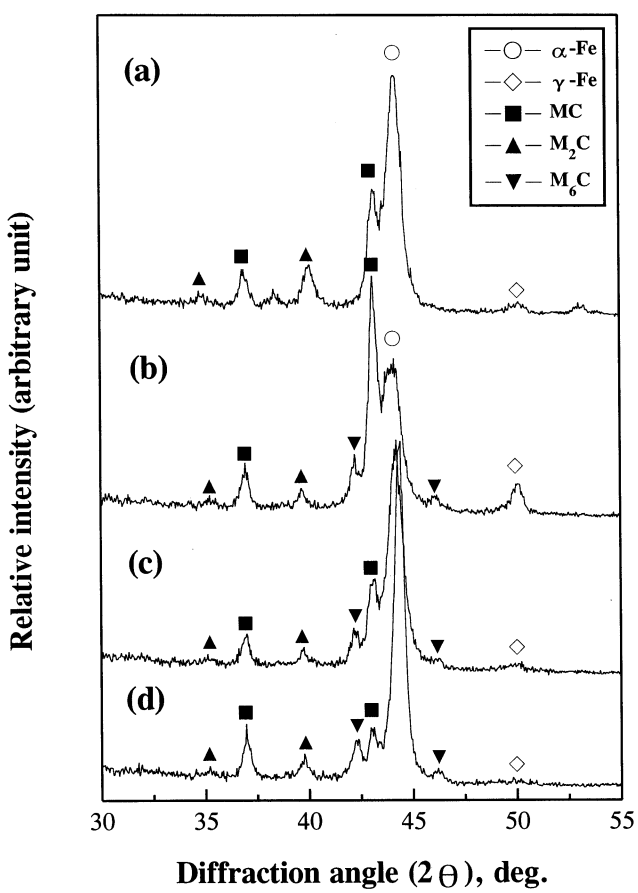

Fig. 6. X-ray diffraction patterns of: (a) the as-cast structure; (b) the structure quenched at 1100°C; (c) the structure quenched at 1100°C and double-tempered at 560°C; and (d) the structure quenched at 1100°C and double-tempered at 635°C for Roll-C2.

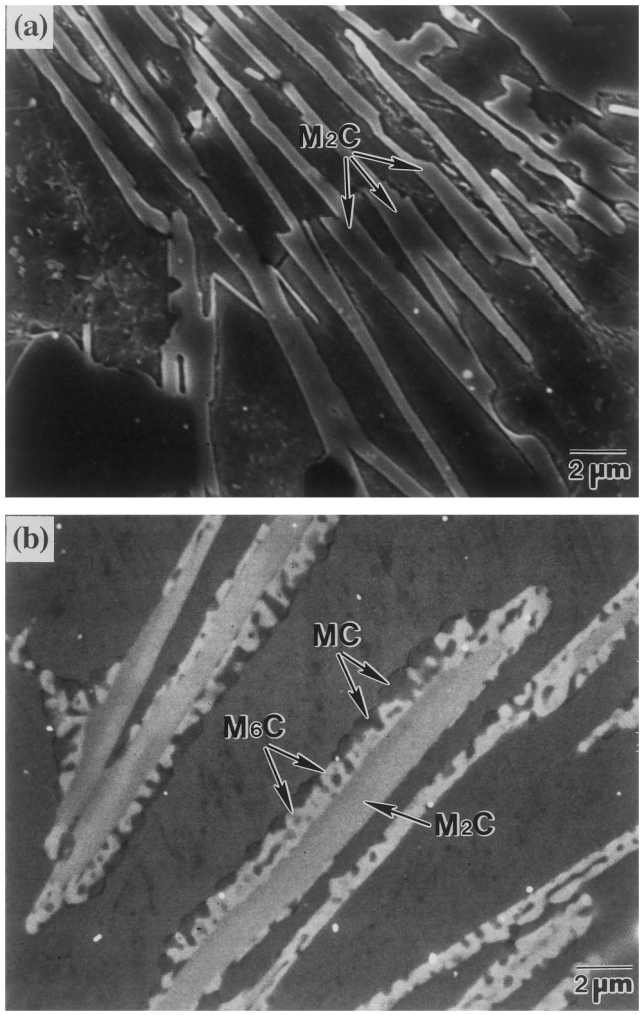

Fig. 7. SEM micrographs of feathery M_2C carbides of: (a) the as-cast structure; and (b) the quenched structure at 1100°C of Roll-C2, showing the decomposition of M_2C eutectic carbides.

The cell sizes of Rolls-C1, and -C2 containing 1.9%C are 89 and 91 μm, respectively, and show an increasing trend with higher tungsten equivalent (Table 4). Primary γ is formed first as the liquid composition starts from Point A, and the liquidus line moves along AB_3. Upon reaching Point B_3, the line moves along $B_3P'_3$, and (γ + MC) eutectic structure is formed independently due to nucleation in the liquid phase. After the retained liquid composition reaches Point P'_3, M_2C carbides are formed in cell boundaries by the peritectic and eutectic reaction of $L + MC \rightarrow \gamma + M_2C$. From these observations, the length of AB_3 line determines the amount of primary γ, while $B_3P'_3$ the amount of (γ + MC) eutectic structure. Comparing with Rolls-B1 and -B2, the cells of Rolls-C1 and -C2 are bigger because line $B_3P'_3$ determining the cell size is longer than $B_2P'_2$. $P_3P'_3$ line gets longer with increasing tungsten equivalent, therefore, the cells get larger in the order of Rolls-C1 and -C2. The fraction of MC carbides in Rolls-C1 and -C2 is considerably high at 10–12% because much more MC carbides can be formed due to the long interval of $B_3P'_3$.

Since the carbon content added to Roll-D is 1.45%, solidification starts from a left side of Point A. It takes longer for primary γ and (γ + MC) eutectic structure to grow, causing cells to grow big up to about 110 μm. The fraction of MC carbides is about 8%, lower than in Rolls-C1 and -C2, due to the comparatively lower fraction of MC carbides.

These analyses based on the liquidus surface diagrams indicate that hardness and fracture toughness can be enhanced simultaneously in the following reasoning: (1) When rolls are designed in such a way to make AB_3 line short while B_3P_3 long (i.e., closer to Point P_3), more MC carbides are formed inside cells; and (2) when the liquidus line arrives at Point P'_3, a small amount of liquid phase is formed by the peritectic and eutectic reaction, reducing the fraction of carbides formed in cell boundaries. Based on these analyses, the effects of each alloying element on microstructure and properties are described in the following section.

4.2. Effects of alloying elements

4.2.1. Carbon

The carbon content in the matrix determines the characteristics of the matrix. As can be seen in the chemical compositions of the HSS rolls in Table 1, the carbon content is about 1.5–2.0%, most of which forms carbides by combining with V, W, Mo, and Cr, while the retained carbon of about 0.2–0.7% is contained inside the matrix, forming plate or lath martensite. When the carbon content is less than 0.3%, it diminishes the heat-treatment effect; but in the case of over 0.6%, it may seriously harm fracture toughness because of the increased amount of plate martensite [6]. The matrix carbon content is shown in Table 4, from which it can be learned that the matrix of Rolls-A, -C1, and -C2 consists of plate martensite, whereas other rolls of mainly lath martensite with a little plate martensite as can be confirmed by Fig. 1(a) through (f). The matrix carbon content is also proportional to the amount of retained austenite because retained austenite tends to form together with plate martensite [6].

When the carbon content is low like in Roll-D (1.45%C), the fraction of MC carbides is about 8%. Comparing them with Roll-C2 which have same chemical compositions except the carbon content, Roll-D tends to show decreasing overall hardness (Table 5). This is because the smaller amount of MC carbides forms and the matrix carbon content is lower; thus, forming mostly lath martensite. However, when the carbon content considerably exceeds a proper amount

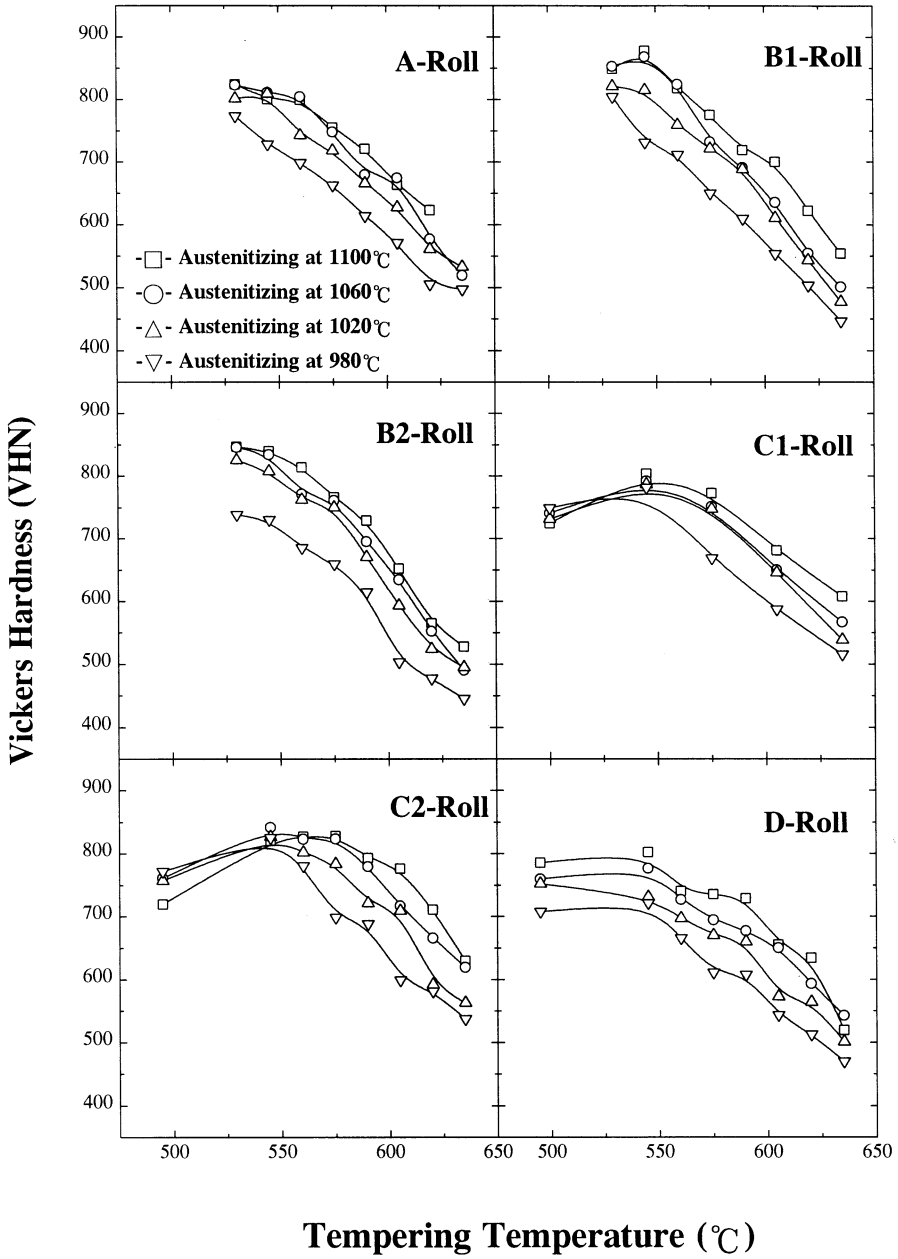

Fig. 8. Vickers hardness vs tempering temperature for all the rolls.

of carbide forming elements, plenty of network-like eutectic structures are formed in cell boundaries. This can also harm hardness and fracture toughness due to the formation of M_3C carbides having low hardness via $L \rightarrow \gamma + M_3C$ reaction [16]. Thus, the carbon content is recommended to satisfy the following carbide stoichiometry depending on the amount of each carbide former [17]:

$$C\% = 0.060Cr\% + 0.063Mo\% + 0.033\%W + 0.235\%V$$

From this formula, the appropriate level of carbon content in the HSS rolls is 1.9–2.0%.

4.2.2. W and Mo

The similarity of roles that W and Mo play in the HSS rolls as carbide formers, therefore, it is rationalized to consider their effect in terms of tungsten equivalent. An appropriate amount of W and Mo improves the distribution of carbides, particularly MC. When they are added excessively, they are excreted into the retained liquid phase during solidification, and accelerate the eutectic reaction. As a result, a large amount of M_2C carbides is formed in cell boundaries. In Rolls-C1 and -C2 containing the high contents of W and Mo, a considerably large amount of M_2C carbides is formed

along cell boundaries (Fig. 3(d) and (e)). On the contrary, when W and Mo are contained very little as in Roll-A, hardness drops because M_2C carbides are hardly formed, and the secondary hardening effect during tempering diminishes. Therefore, the appropriate content of W and Mo is 3–4%, at which the formation of M_2C carbides can be prevented, while homogeneously distributing lots of MC carbides. It is further recommended to lower the ratio of W/Mo so that fracture toughness can be improved by forming the lath martensitic matrix.

4.2.3. Cr

The Cr addition prevents oxidization on the roll surface, improves hardness of the matrix by precipitating fine carbides, and helps form iron oxide layers on the roll surface during hot rolling. Thus, it is added to the HSS rolls, in general, at over 5%. Excessive content of Cr, however, deteriorates fracture toughness since much of Cr causes the formation of many M_7C_3 carbides mainly in cell boundaries. In Rolls-B1 and -B2 containing 9% Cr, lots of M_7C_3 carbides (about 15%), instead of MC carbides, are formed in cell boundaries. Therefore, the appropriate Cr level is 5–7%, which can be modified considering the effect of iron oxide layers on the roll surface in actual applications.

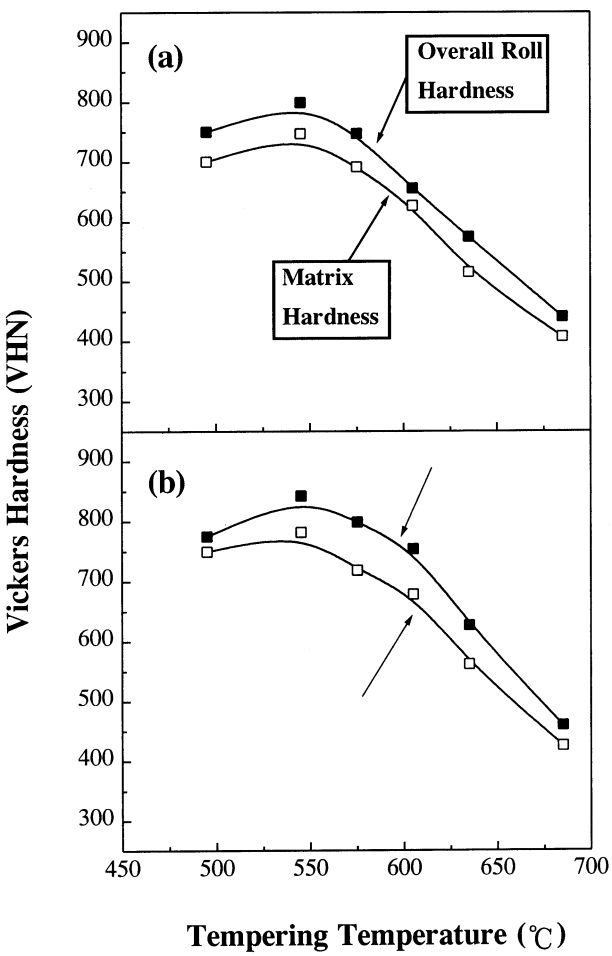

Fig. 9. Vickers hardness vs tempering temperature for: (a) Roll-C1; and (b) Roll-C2; showing the comparison between the overall hardness and the matrix hardness. All the rolls were quenched at 1060°C prior to double-tempering.

4.2.4. V

When combined with carbon, V forms very hard MC carbides, improving hardness and wear resistance. If the contents of W, Mo, and Cr are fixed in the liquidus surface diagram of Fig. 10, each liquidus line is accordingly fixed. When the V content is low under a certain carbon content, the interval to form primary γ is lengthened, causing MC carbides to form under insufficient amount of liquid phase; hence, resulting in the segregation of MC carbides in cell boundaries. For example, in Roll-B1 containing 3.6% V, the fraction of MC carbides is only 2.2% (Table 4), most of which is distributed in cell boundaries (Fig. 1(b)). Rolls with such a carbide distribution as this might show relatively low fracture toughness in spite of low fraction of carbides. On the other hand, an excessive level of V beyond the γ/MC boundary of Fig. 10 causes MC carbides to initially form, not γ phase. MC carbides having lower density (5.6 g cm^{-3}) than liquid phase tend to be segregated toward the central part of the rolls by centrifugal force during casting, significantly reducing the V adding effect. Accordingly, the appropriate V content is found to be about 5–6%, raised up to the γ region near the triple junction of δ-γ-MC in the Fe–5Cr–5W–5Mo–V–C system of Fig. 10. In this case, MC carbides are formed in a state with sufficient liquid phase, grow together with primary γ, and are homogeneously distributed mainly inside cells.

The aforementioned results indicate that the appropriate contents of alloying elements are 1.9–2.0% for carbon, 3–4% for W and Mo respectively, 5–7% for Cr, and 5–6% for V. However, the appropriate content of each alloying element can vary depending on the interaction with other alloying elements and on the actual rolling conditions applicable to roll stands. Although the increasing carbide fraction improves hardness, wear resistance, and roughness, the excessive fraction might cause the rolling force to rise, and promote sticking phenomenon in rolls and rolled plates; hence, careful attention should be paid in determining the appropriate alloying contents. The alloy design should also be considered to form iron oxide layers steadily on the roll surface. The present study intends to interpret the effects of alloying elements on microstructure and mechanical properties via alloy design, and suggests that the most critical microstructural factors affecting properties are the fraction and distribution of carbides. The alloy design of the HSS rolls to

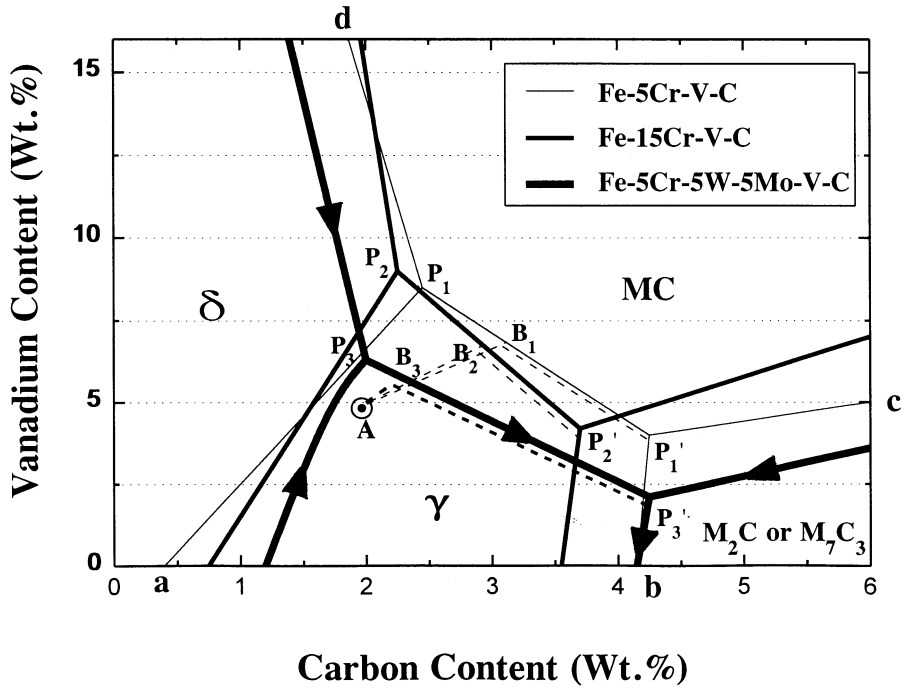

Fig. 10. Liquidus surface diagram of Fe–5Cr–V–C, Fe–15Cr–V–C, and Fe–5Cr–5W–5Mo–V–C alloy systems [16].

improve mechanical properties is very essential to the actual application of the rolls, therefore, continuous studies should be made on the optimization of casting process, enhancement of carbide distribution, reduction of rolling force, the mechanism of fracture and thermal fatigue phenomenon, and the analysis of iron oxide layers and their stabilization.

4.3. Cooling rate

The cooling rate during casting affects the carbide formation. Fig. 11(a) through (c) are optical micrographs showing the changes in carbides as to the distance from the surface of Roll-C2. In the surface region, a number of fibrous M2C carbides are observed (Fig. 11(a)). As it gets into the interior, M_6C carbides are formed, while the fraction of M_2C carbides is reduced (Fig. 11(b) and (c)). This indicates that many M_2C carbides are formed at faster cooling rate, whereas M_6C carbides, together with M_2C carbides, are formed at slower rate.

At a given cooling rate, the matrix characteristics are changed depending on the composition. For instance, in the matrix of Roll-A, to which only a small amount of alloying elements is added, pearlite is formed because the cooling curve meets probably with the pearlite nose during cooling. If the nose moves to the right as in Rolls-B1 through -D due to the high contents of W, Mo, Cr, and V in the matrix, phase transformation to martensite occurs readily because the cooling curve does not meet with the pearlite nose.

5. Conclusions

In this study, the effects of alloying elements on microstructure and fracture properties of six HSS rolls manufactured by centrifugal casting method was investigated.

1. The as-cast HSS rolls consist of the martensitic matrix, hard carbides such as MC, M_2C, M_7C_3, and M_6C, and fine carbides inside the matrix. The most important microstructural factor among them is the intercellular carbides and their distribution.
2. Various types of carbides are formed depending on the contents of strong carbide forming elements. In Rolls-A, -B1, and -B2 containing the high Cr content, MC carbides inside cells and M_7C_3 carbides in cell boundaries are primarily formed. In Rolls-Cl, -C2, and -D containing the high W and Mo contents, MC carbides inside the cells and fibrous M_2C carbides in the intercellular regions are dominantly formed, with additional formation of M_6C carbides in Roll-D.
3. The carbon content of the matrix is 0.2–0.7%. The matrix type is mainly lath one when the carbon content is under 0.4%, while mainly plate one when it is over 0.4%. Overall roll hardness tends to increase when the martensitic matrix is of plate-type and as the total carbide fraction increases.
4. The effects of alloying elements are analyzed using the liquidus surface diagram showing the solidification process of the HSS rolls. The results of the appropriate content of each alloying element are; 1.9–2.0% of carbon, 3–4% of W and Mo, respectively, 5–7% of Cr, and 5–6% of V.

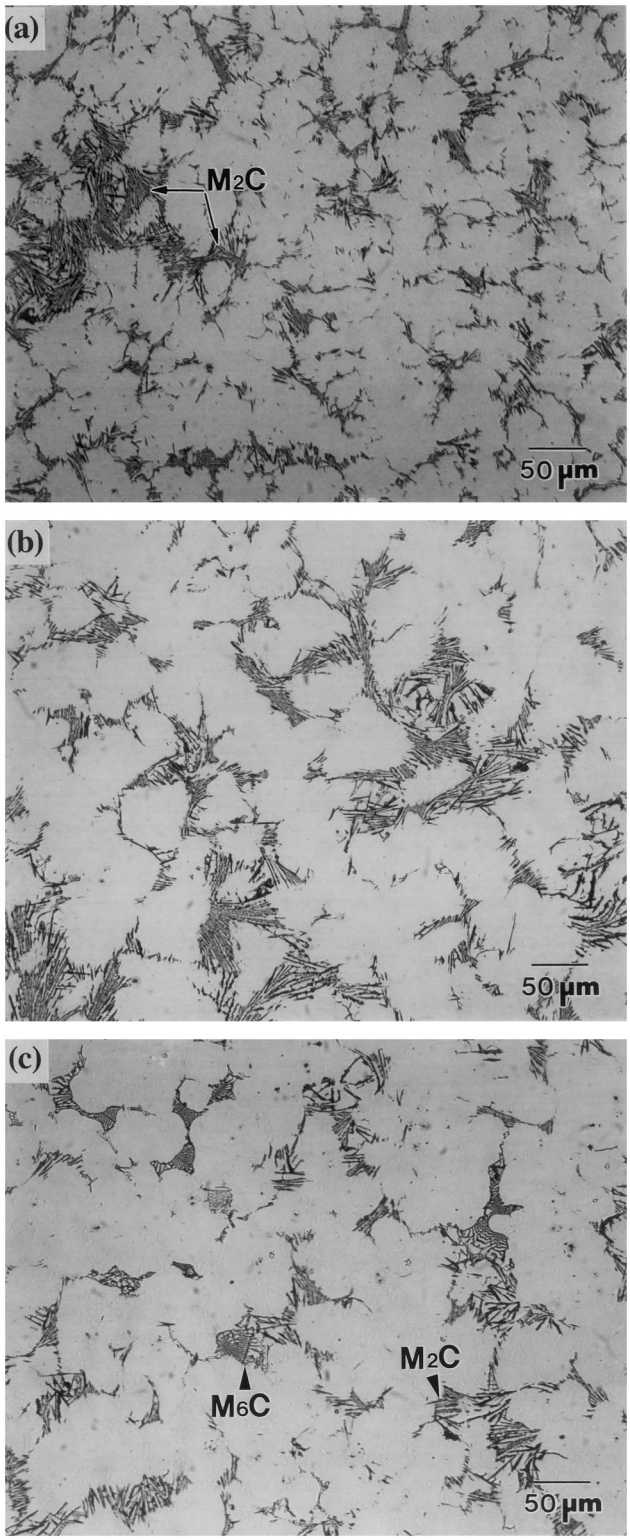

Fig. 11. Optical micrographs of as-cast Roll-C2, showing eutectic carbides in the regions: (a) 10 mm; (b) 35 mm; and (c) 60 mm away from the roll surface. Etched by Murakami etchant.

5. In the heat-treated rolls, no variations in the fraction and distribution of carbides are found, except that M_2C carbides are decomposed to MC and M_6C carbides, while the matrix is changed to mostly plate-type tempered martensite. The heat-treated rolls have higher hardness as the austenitization temperature increases, and show peak hardness at 525°C for Rolls-A, -B1, and -B2 and at 550°C for Rolls-C1, -C2, and -D. The secondary hardening effect is not obvious.

Acknowledgements

This work has been supported by Kangwon Industries. The authors thank Dr Eon Sik Lee of Research Institute of Industrial Science and Technology, Professor Nack J. Kim of POSTECH, and Vice President Hee Seung Han and Byung Il Jung of Kangwon Industries, for their helpful discussion on microstructural analysis of the HSS rolls.

References

[1] J.C. Werquin, J.C. Caillaud, in: R.B. Corbett (Ed.), Rolls for the Metal Working Industries, Iron and Steel Society, Warrendale, PA, 1990, ch. 4.
[2] W.H. Betts, H.L. Baxter, in: R.B. Corbett (Ed.), Rolls for the Metal Working Industries, Iron and Steel Society, Warrendale, PA, 1990, ch. 2.
[3] Y. Sano, T. Hattori, M. Haga, ISIJ Int. 32 (1992) 1194.
[4] T. Kudo, S. Kawashima, R. Kurahashi, ISIJ Int. 32 (1992) 1190.
[5] K. Goto, Y. Matsuda, K. Sakamoto, Y. Sugimoto, ISIJ Int. 32 (1992) 1184.
[6] R. Honeycombe, H.K.D.H. Bhadeshia, in: Eward Arnold (Ed.), Steels-Microstructure and Properties, London, 1995, ch. 5.
[7] S.J. Manganello, in: R.B. Corbett (Ed.), Rolls for the Metal Working Industries, Iron and Steel Society, Warrendale, PA, 1990, p. 227.
[8] J.J. deBarbadillo, C.J. Trozzi, Iron and Steel Engineer 1 (1981) 63.
[9] L.A. Dobrzanski, Steel Res. 57 (1986) 37.
[10] G.L.F. Powell, P.G. Lloyd, Metallography 14 (1981) 271.
[11] S. Karagoz, H. Fischmeister, Steel Res. 58 (1987) 46.
[12] E. Haberling, A. Rose, H.H. Weigand, Stahl Eisen 93 (1973) 645.
[13] W.F. Smith, Structure and Properties of Engineering Alloys, McGraw-Hill, 1981, ch. 1, ch. 9.
[14] W.C. Leslie, The Physical Metallurgy of Steels, McGraw-Hill, 1981, ch. 8.
[15] M. Hashimoto, S. Otomo, K. Yoshida, K. Kimura, R. Kurahashi, T. Kawakami, T. Kouga, ISIJ Int. 32 (1992) 1202.
[16] K. Ogi, Imono 66 (1994) 764.
[17] Y. Matsubara, N. Sasaguri, Y. Honda, H. Wu, M. Hashimoto, Imono 66 (1994) 815.